Linear and Four-Armed Poly(L-lactide)-*block*-poly(D-lactide) Copolymers and Their Stereocomplexation with Poly(lactide)s

Jun Shao,[1,2] Zhaohui Tang,[1] Jingru Sun,[1] Gao Li,[1] Xuesi Chen[1]

[1]Key Laboratory of Polymer Ecomaterials, Changchun Institute of Applied Chemistry, Chinese Academy of Sciences, Changchun 130022, China
[2]College of chemistry and chemical engineering, JiangXi Normal University, Nanchang 330022, China
Correspondence to: G. Li (E-mail: ligao@ciac.ac.cn) or X. Chen (E-mail: xschen@ciac.ac.cn)

Abstract: Linear and four-armed poly(L-lactide)-*block*-poly(D-lactide) (PLLA-*b*-PDLA) block copolymers are synthesized by ring-opening polymerization of D-lactide on the end hydroxyl of linear and four-armed PLLA prepolymers. DSC results indicate that the melting temperature and melting enthalpies of poly(lactide) stereocomplex in the copolymers are obviously lower than corresponding linear and four-armed PLLA/PDLA blends. Compared with the four-armed PLLA-*b*-PDLA copolymer, the similar linear PLLA-*b*-PDLA shows higher melting temperature (212.3 °C) and larger melting enthalpy (70.6 J g^{-1}). After these copolymers blend with additional neat PLAs, DSC, and WAXD results show that the stereocomplex formation between free PLA molecular chain and enantiomeric PLA block is the major stereocomplex formation. In the linear copolymer/linear PLA blends, the stereocomplex crystallites (sc) as well as homochiral crystallites (hc) form in the copolymer/PLA cast films. How-

ever, in the four-armed copolymer/linear PLA blends, both sc and hc develop in the four-armed PLLA-*b*-PDLA/PDLA specimen, which means that the stereocomplexation mainly forms between free PDLA molecule and the inside PLLA block, and the outside PDLA block could form some microcrystallites. Although the melting enthalpies of stereocomplexes in the blends are smaller than that of neat copolymers, only two-thirds of the molecular chains participate in the stereocomplex formation, and the crystallization efficiency strengthens. © 2014 Wiley Periodicals, Inc. J. Polym. Sci., Part B: Polym. Phys. **2014**, *52*, 1560–1567

KEYWORDS: blends; branched poly(lactide); crystallization behavior; poly(lactide); poly(lactide) stereo-block copolymers; poly(lactide) stereocomplex

INTRODUCTION Poly(lactide) (PLA) is one of the most important bioplastics; it is extensively studied for medical and engineering applications because of its renewability, biodegradability, biocompatibility, and mechanical properties.[1–3] However, compared with traditional polymers, the thermal distortion temperature of PLA is poor for applications.[4,5] Depending on the optical isomer of the lactic acid, PLA has two enantiomers, poly(L-lactide) (PLLA) and poly(D-lactide) (PDLA). Mixing of PLLA and PDLA gives rise to the formation of PLA stereocomplex crystallites (sc), which are different from homochiral crystallites (hc) formed in PLLA or PDLA.[6] Since PLA sc shows a higher melting temperature, ∼220 °C, and higher crystallization speed than neat PLLA and PDLA, the PLA stereocomplex materials present dramatically improved thermal properties.[7,8] Notwithstanding, the PLA hc along with sc always forms in the PLLA/PDLA blend with high molecular weights, which reduces the thermal resistance temperature.[9,10] Accordingly, lots of investigations are focused on improving the stereocomplex efficiency, such as adding shearing field,[10] controlling the temperature during melting blend-

ing,[11] varying the annealing temperature,[12] changing the structure of the blends,[13–15] and adopting super critical condition.[16,17] The PLLA-*b*-PDLA stereoblock copolymer is also commonly used in the PLLA/PDLA blends for obtaining efficiently stereocomplexed materials.[18] According to literature, the PLLA-*b*-PDLA stereoblock copolymers can be prepared many ways: (1) first the PLLA (or PDLA) prepolymer is synthesized, followed by D-LA (or L-LA) ring opening polymerization on the end hydroxyl group of prepolymers,[19–22] (2) functionalized PLLA reacts to modified PDLA,[23] (3) PLLA-*b*-PDLA multi-block copolymer can be obtained by solid-state polycondensation of PLLA with PDLA at relative low molecular weights,[24,25] or stereoselective polymerization of the racemic lactide.[26,27] (4) the cyclic PLLA-*b*-PDLA copolymers are developed by adopting a coupling reaction.[28] In the past two decades, multi-armed polymers have attracted attention because of their unique physical and chemical properties and particular topological structures.[5,29–34] The stereocomplex formation between multiarmed PLLA and PDLA were also investigated.[13–15,35–38] Recently, Isono *et al* prepared the star-shaped
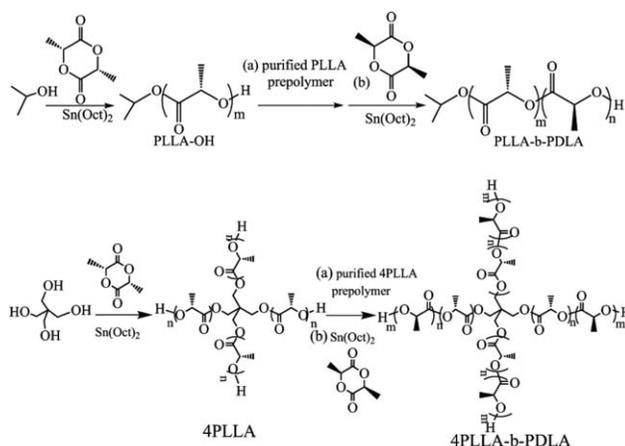
SCHEME 1 Synthesis of linear and four-armed PLLA and PLLA-b-PDLA

PLA copolymer, which has both PLLA and PDLA arms in one macromolecule.[39] Among these numerous reports on the synthesis of stereoblock PLLA-b-PDLA, little attention has been paid to the properties of star shaped PLLA-b-PDLA copolymers, and the differences between linear and multiarmed PLLA-b-PDLA copolymers are still unclear. Furthermore, in the blend of linear and 4-armed PLLA-b-PDLA/PLAs, the stereocomplexation will form between the PLLA block and PDLA block, and between the free PLA chain and enantiomeric PLA block. However, there has been no research focus on the case for which stereocomplex formation is predominant, and this is very important for the application of PLLA-b-PDLA. In addition, in the four-armed PLLA-b-PDLA block copolymer/PLLA blend, when the stereocomplexation occurs between free PLLA chains and the outside PDLA block, the crystallization of the inside PLLA block will be confined by the outside stereocomplex crystallites and the inside core, and its crystallization behavior has been ambiguous until now.

In this work, the linear and four-armed PLLA-b-PDLA copolymers were synthesized and then blended with PLAs with different configurations. The crystallization behaviors of these copolymers and their blends were investigated in detail. The results indicated that the melting temperature and enthalpy of stereocomplex crystallites in the PLLA-b-PDLA were lower than corresponding PLLA/PDLA blends, and the crystallinity of the PLLA-b-PDLA/PLA blends were lowest among the PLLA-b-PDLA and PLLA/PDLA specimens. This investigation will provide some guidance in the application of PLLA-b-PDLA and its blends with PLA.

EXPERIMENTAL

Materials

D-Lactide (D-LA) and L-lactide (L-LA), optical purities $\geq 99.5\%$, were bought from Changchun Sino Biomaterials (China), and they were recrystallized from dry acetic ether for three times, respectively. Tin (II) ethylhexanoate [$Sn(Oct)_2$, 95%] was purchased from Aldrich and was used without purification. Toluene was refluxed with sodium to dehydrate before

distillation. 1,1,1,3,3,3-Hexafluoro-2-propanol (HFIP, $\geq 99\%$) was supplied from DuPont (USA) and was refluxed with calcium hydride before used. Isopropanol was refluxed with calcium hydride. Pentaerythritol was dried by azeotropic distillation in dry toluene. All these materials preserved in an inert atmosphere after purification.

Synthesis of Linear and Four-Armed PLLA and PLLA-b-PDLA

The synthesis routes of linear, four-armed PLLA and corresponding PLLA-b-PDLA block copolymers present in Scheme 1. The linear PLLA and PDLA were synthesized by the ring-opening polymerization of L-LA and D-LA in toluene solution at the presence of isopropanol and $Sn(Oct)_2$ as literatures.[15,40] The four-armed PLLA and PDLA (4PLLA, 4PDLA) were initiated by pentaerythritol as reports.[41,42] All the obtained polymers were purified by repeated dissolution and precipitation. Dichloromethane and methanol were used as solvent and precipitant, respectively. The prepolymer products were dried in vacuum at room temperature at first, then at 60 °C in vacuum to constant weight. The characterizations of neat polymers listed in Table 1.

The synthesis of linear and four-armed PLLA-b-PDLA copolymers were according to the literatures.[20] Dried PLLA and 4PLLA, given D-lactide, and $Sn(Oct)_2$ were dissolved in toluene, sealed in ampoule under nitrogen atmosphere, and then the ring-opening polymerization of D-lactide was performed at 120 °C in toluene for 96 h. The obtained copolymers were dissolved in a mixed solvent of dichloromethane/HFIP (v/v = 90/10), and then precipitated in methanol. The dissolution and precipitation repeated for twice. The purified block copolymers were dried as the same method as prepolymers.

Preparation the Blends and Neat Specimens

The casted films used for physical measurements were prepared with the method described in literatures.[10,15] Linear and four-armed PLLA-b-PDLA block copolymers were dissolved in dichloromethane/HFIP mixed solution, respectively. PDLA, PLLA, 4PDLA, and 4PLLA were dissolved in dichloromethane, separately. All the concentrations of solutions were 10.0 g L^{-1}. The copolymers and neat PLA solutions were admixed under vigorous stirring for 3 h, and the mixing molar ratio of the blends fixed at 1:1. After that, the mixed solutions were casted onto petri-dishes, followed by solvent

TABLE 1 Characterization of Neat PLA

Code	M_n[a] (kg mol^{-1})	PDI[a]	T_{hm}[b] (°C)	ΔH_{hm}[b] (J g^{-1})
L15	14.7	1.1	165.5	67.2
D14	14.4	1.1	166.8	69.1
4L60	60.4	1.3	166.1	47.3
4D61	60.8	1.3	167.4	45.4

[a] The M_n was calibrated as polystyrene standard in chloroform.
[b] The T_{hm} and ΔH_{hm} was the melting temperatures and enthalpies of PLA homocrystallites during the first heating under a heating rate of 10 °C min^{-1}.

TABLE 2 Characterization of PLLA Prepolymer and Block Copolymer

Code	D-LA/PLLA (W/W)	M_n[a] (kg mol^{-1})	PDI[a]	$[\alpha]_{20}$[b] deg cm^3/ (dm^{-1} g^{-1})	D Content[c] (%)
L15	0	20	1.4	−247.0 ± 2.9	0
sb-L15-1	0.55/1	27	1.5	−137.1 ± 0.9	22.2 ± 0.2
sb-L15-2	1.05/1	32	1.6	−23.5 ± 1.7	45.2 ± 0.3
4L60	0	72	1.3	−240.7 ± 0.8	0
sb-4L60-2	1.05/1	126	2.0	+8.5 ± 0.9	51.8 ± 0.2

[a] The molecular weight and *PDI* were calculated by GPC calibrated by PMMA.
[b] All the prepolymers and copolymers were dissolved in HFIP.
[c] D content was calculated by the optical rotation.

evaporation at room temperature. For comparison, the PLLA, PLLA/PDLA 4PLLA, 4PLLA/4PDLA, linear, and neat four-armed PLLA-*b*-PDLA copolymers cast films were prepared as the same method, respectively. All the films dried at room temperature for a week, and then dried to constant weight at 55 °C.

Characterizations

The number (M_n) and weight-average (M_w) molecular weights were determined by gel permeation chromatography (GPC) with a Waters analyzer system comprising a waters 515 HPLC pump, a waters 2414 refractive index detector, and a Bio as system data processor. For neat PLA specimens, the chloroform was selected as elution solution with two Styragel® HR gel columns (HR2 and HR4). The temperature were fixed at 35 °C, and the molecular weights were calibrated with polystyrene. The neat polymers were listed in Table 1. For PLA prepolymers and copolymers, HFIP was used as the elute solution at 30 °C through a copolymer gel column, Shodex HFIP-806 (8.0 × 300 mm^2). The molecular weights were calibrated as poly(methyl methacrylate) (PMMA) standards. The characterization of prepolymers and copolymers showed in Table 2.

The specific optical rotation ($[\alpha]_{20}^{589}$) of the polymers were measured in HFIP solution at a concentration of 1.0 g L^{-1} at 20 °C, using 341LC polarimeter (Perkin Elemr) with a sodium lamp at a wave length of 589 nm. The L-lactyl unit content of PLLA-*b*-PDLA copolymers was calculated by the following equation:[20]

$$\text{L lactyl unit content}(\%) = 100 \times \frac{[\alpha]_{20}^{589} + [\alpha]_{20}^{589}(\text{PLLA})}{2 \times [\alpha]_{20}^{589}(\text{PLLA})} \quad (1)$$

where $[\alpha]_{20}^{589}(\text{PLLA})$ was the optical rotation value for linear and four-armed PLLA prepolymer, respectively, and the $[\alpha]_{20}^{589}$ values were the optical rotations of linear and four-armed PLLA-*b*-PDLA copolymers.

The thermal properties of prepolymers, copolymers, and blends were examined by differential scanning calorimeter

(DSC; Q100, TA Instruments). The temperature and heat flow were calibrated with standard indium ($T_m = 156.6$ °C and $\Delta H = 28.5$ J g^{-1}). DSC scans were carried out under nitrogen atmosphere from 20 to 200 °C, 20 to 240 °C, and 20 to 250 °C for neat PLAs, copolymers, and blends, respectively, and the scans were recorded at a rate of 10 °C min^{-1} to compare the melting temperature and fusion enthalpy of the different samples.

Wide angle X-ray diffraction (WAXD) measurements were carried out on a Bruker D8 Advance X-ray diffractometer, equipped with Cu Kα radiation, the measurement running at a scan speed of 2° min^{-1}, and scattering angle ranged from $2\theta = 10°$ to 30°.

RESULTS AND DISCUSSION

Characterizations of PLA Prepolymers and Copolymers

The synthesis route of linear and four-armed PLLA and PLLA-*b*-PDLA copolymers is shown in Scheme 1, and the characterization of prepolymers and copolymers are listed in Table 2. In the table, the linear PLLA is separately coded as L, and the number after it is number average molecular weight calibrated by polystyrene standard. The linear PLLA-*b*-PDLA block copolymer is coded as sb-L. For the four-armed PLLA and copolymers, they are coded as 4L and sb-4L, respectively.

The molecular weight increased as the D-LA/PLLA weight ratio increasing after the copolymerization, but the molecular weight distribution became wider, which indicated that the PDLA block was not as uniform as the PLLA prepolymers, especially for the four-armed copolymer. During the copolymerization, the stereocomplexation formed between PDLA and PLLA blocks in toluene, and the stereocomplexed PLA precipitated from the solution. The copolymerization was not controllable exactly as the copolymerization in bulk as in the literature.[19,20] From Table 2, it can been seen that the optical rotation decreased gradually as D-LA addition increased, although the D resultant content in copolymers did not correlate with the D-LA feed ratio strictly, which should be assigned to the stereocomplex formation between the PDLA and PLLA block that hindered the copolymerization. The measured molecular weight of PLLA (L15) was 15 kg mol^{-1} in chloroform (Table 1), but this value became 20 kg mol^{-1} in HFIP (Table 2), which should be due to the different standards and the elution solvent adopted in the two measurements.

Thermal Properties of PLLA, PLLA-*b*-PDLA, and PLLA/PDLA Blends

The DSC of PLLA, PLLA-*b*-PDLA, and PLLA/PDLA specimens can be seen in Figure 1, and its data of the first heating were collected in Table 3. From the first scanning [Fig. 1(a)], the melting temperature of PLA hc (T_{hm}) in L15 is observed at 165.5 °C, while it decreased to 159.7 °C in sb-L15-1, and disappeared in the specimen of sb-L15-2. However, another endothermic peak above 180 °C appeared in the copolymers, which is attributed to the melting of PLA sc. The melting
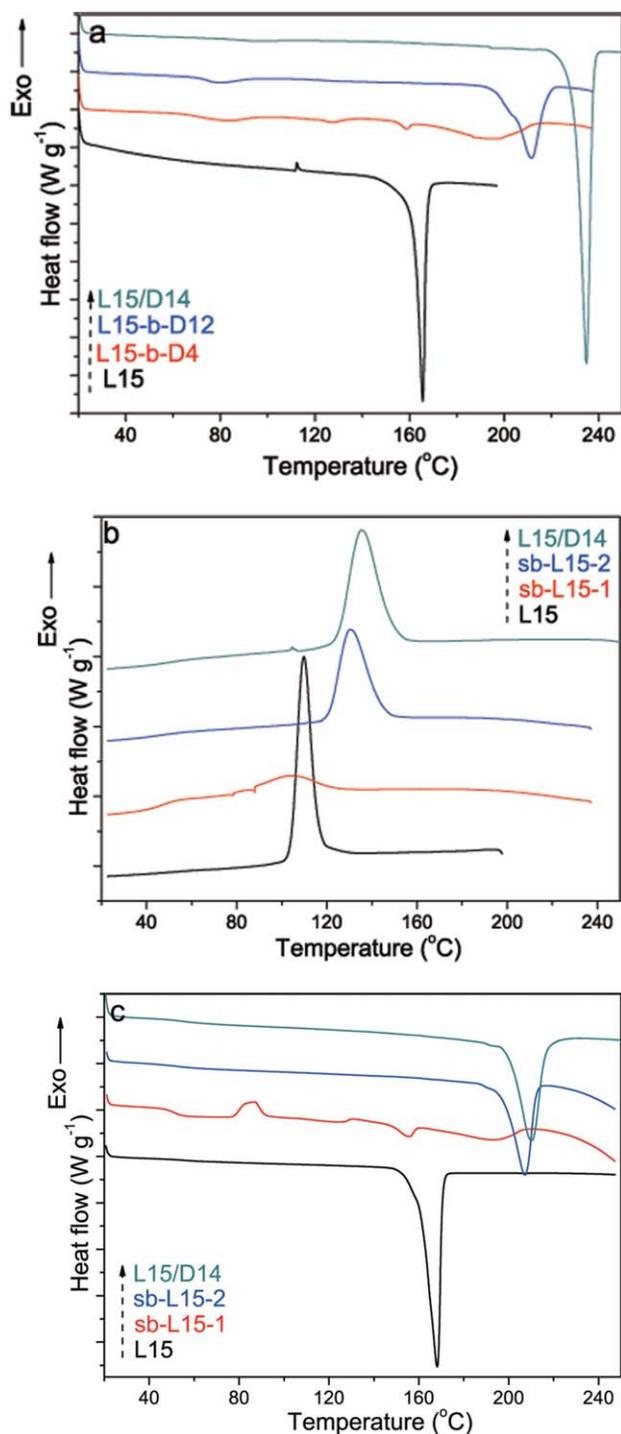
FIGURE 1 DSC of L15, sb-L15-1, sb-L15-2, and L15/D14. (a) First heating, (b) cooling, and (c) second heating. [Color figure can be viewed in the online issue, which is available at wileyonline-library.com.]

temperature (T_{sc}) and enthalpy (ΔH_{sc}) of PLA sc increased as the D content increased. In the L15/D14 blend, only one endothermic peak at 235.0 °C belonging to sc was detected, and the ΔH_{sc} (108.9 J g^{-1}) was much higher than those of the copolymers.

TABLE 3 Data Collected from the DSC of the Binary Blends

Code	T_{hm} (°C)	ΔH_{hm} (J g^{-1})	T_{sc} (°C)	ΔH_{sc} (J g^{-1})	Total Crystallinity (%)
L15	165.5	67.2	–	–	72.8
sb-L15-1	159.7	7.7	197.0	23.6	24.8
sb-L15-2	–	–	212.3	70.6	49.7
sb-L15-2/L15	164.1	2.0	213.1	50.5	35.7
sb-L15-2/D14	–	–	225.3	62.1	43.7
L15/D14	–	–	235.0	108.9	76.7
4L60	66.1	47.3	–	–	50.5
sb-4L60-2	–	–	204.5	50.7	35.7
sb-4L60-2/L15	–	–	210.4	40.2	28.3
sb-4L60-2/D14	159.4	0.6	214.5	40.6	29.2
4L60/4D61	–	–	221.9	62.8	44.2

During cooling [Fig. 1(b)], the L15 crystallized at 109.8 °C. In the sb-L15-1, the crystallization temperature (T_c, 103.7 °C) and enthalpy (ΔH_c) were obviously lower than that in L15. The T_c and ΔH_c increased as the D content enhanced in the copolymer. The L15/D14 crystallized at the highest temperature, 135.1 °C. The second heating of the specimens [Fig. 1(c)] was similar to the first heating but slightly lower than the melting temperature of PLA sc. This is likely due to the interdiffusion of the molecules after melting which hindered stereocomplex formation, as well as degradation after melting.

The speculated crystallizations of PLLA, PLLA-*b*-PDLA copolymers, and PLLA/PDLA are depicted in Scheme 2. In neat PLLA, all the molecular chains were homogeneous, and the segments could congregate and form hc rapidly. In the sb-L15-1 specimen, the PDLA block appeared but was much shorter than the PLLA block, and both PLA hc and sc could form. The preferentially formed PLA sc would hinder the formation of hc, and the amorphous homochiral chain would hinder the stereocomplex formation at the same time, as the restriction between different crystallites were reciprocal, leading to the slower crystallization rate and lower crystallinity. For the sb-L15-2, the length of PLLA block was slightly longer than PDLA segment, the stereocomplex ability enhanced, and the redundant PLLA part could not form
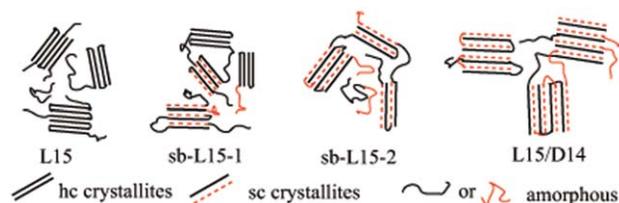
SCHEME 2 The speculated crystallization behaviors of linear PLLA, PLLA-*b*-PDLA copolymer, and PLLA/PDLA blend. [Color figure can be viewed in the online issue, which is available at wileyonlinelibrary.com.]
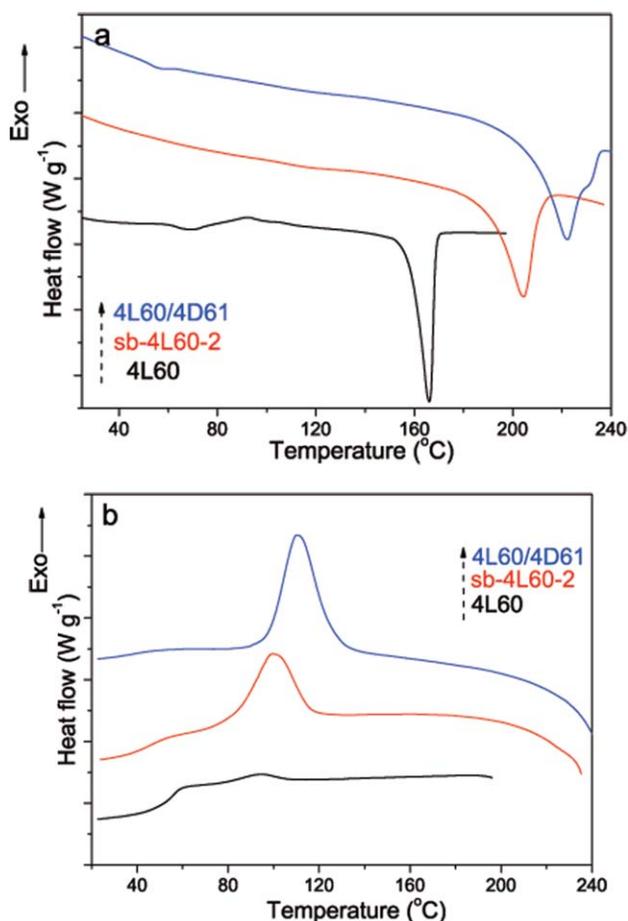
FIGURE 2 DSC of four-armed PLLA prepolymer, copolymer, and blends; (a) first heating and (b) cooling. [Color figure can be viewed in the online issue, which is available at wileyonlinelibrary.com.]

crystallites. Thus, only PLA sc could form, and their crystallization rate and melting temperature enhanced. However, a chemical bond connected the PLLA to PDLA block, which limited the movement of two segments. The PLLA and PDLA molecular chains could move freely in the L15/D14 blend, and the stereocomplexation was more efficient whenever crystallized from the solution and melted state, thus, both the crystallization capacity and melting temperature were the highest in all specimens.

The DSC of 4L60, sb-4L60-2, and 4L60/4D61 is shown in Figure 2. In the first heating [Fig. 2(a) and Table 3], the variations of T_{sc} and ΔH_{sc} of the specimens were similar to corresponding linear polymers. However, the T_{sc} (204.5 °C) and ΔH_{sc} (50.7 J g^{-1}) in sb-4L60-2 were much lower than sb-L15-2, which is also found between the 4L60/4D61 and L15/D14 samples; this was ascribed to the steric hindrance of multi-armed structure, and the restriction from the central core hindered the stereocomplexation. During the cooling [Fig. 2(b)], the 4L60 formed few crystallites, but the sb-4L60-2 and 4L60/4D61 crystallized at higher temperatures and formed larger enthalpies, which could be interpreted

that the four-armed structure hindered the crystallization of each branched PLLA, but the strong hydrogen bond interaction between PLLA and PDLA segment accelerated the formation of crystallites.[43] The second heating of these specimens was similar to the first heating and is not discussed here.

Thermal Properties of PLLA-*b*-PDLA/PLLA Blends

To compare the thermal properties of neat copolymer and copolymer/PLA blends, the sb-L15-2, and sb-4L60-2 were selected and their blends with linear PLAs were prepared.

Sb-L15-*b*-2/PLAs

Figure 3(a) presents the DSC of sb-L15-2 and its blends (first heating), and the results are listed in Table 3. Only one endothermic peak (212.3 °C) assigned to PLA sc was found in the sb-L15-2. When the sb-L15-2 blended with L15, the T_{sc} did not change obviously but slightly reduced the ΔH_{sc}. Additionally, another peak observed around 164 °C is ascribed to the melting of PLA hc. In sb-L15-2/D14 specimen, one clear endothermic peak at 225.3 °C presented, which is assigned to the melting of PLA sc, and its ΔH_{sc} was higher than that of sb-L15-2/L15.
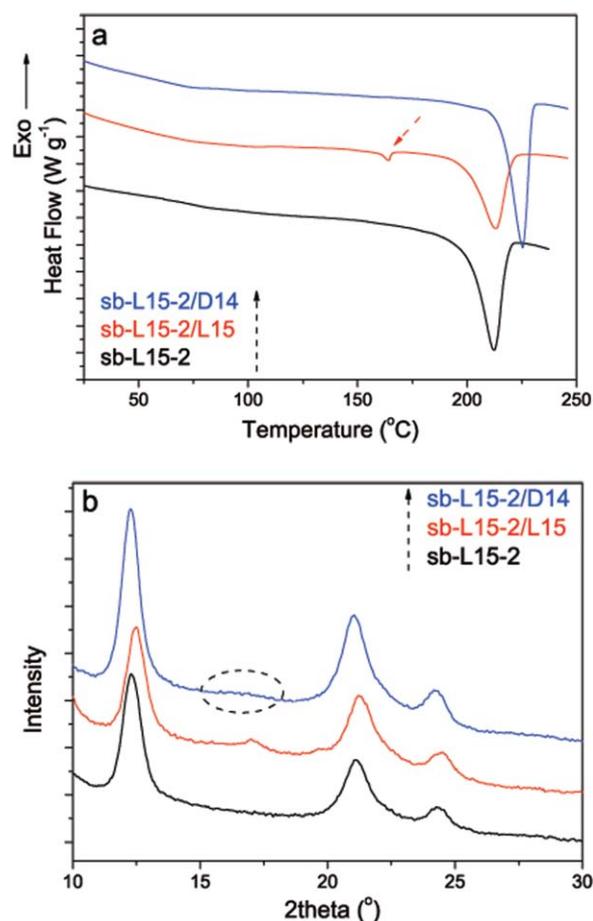
FIGURE 3 The DSC (a) and WAXD (b) of sb-L15-2, sb-L15-2/L15, and sb-L15-2/D14. [Color figure can be viewed in the online issue, which is available at wileyonlinelibrary.com.]
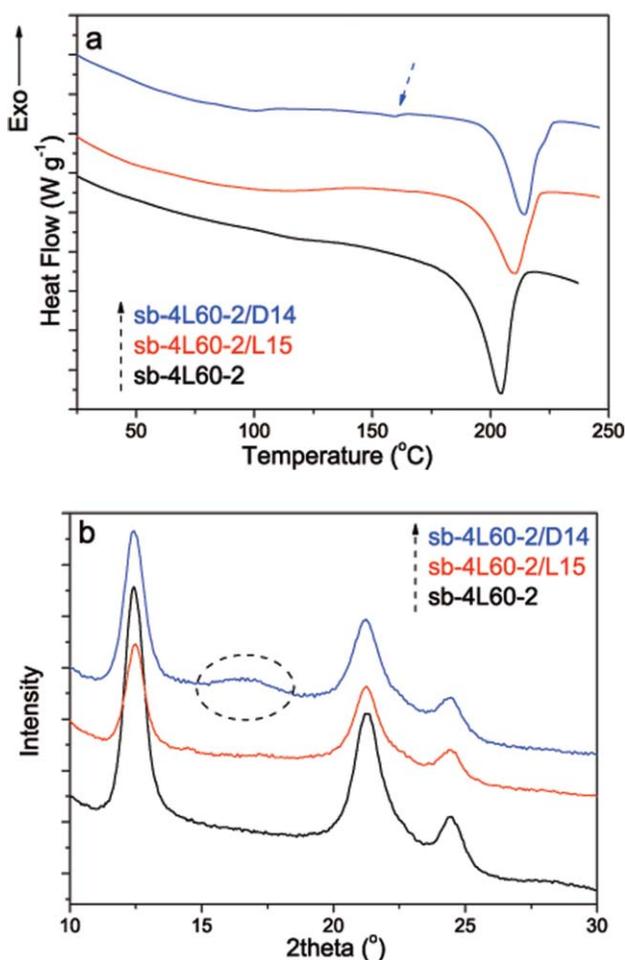
FIGURE 4 The DSC (a) and WAXD (b) of sb-4L60-2 and its blends. [Color figure can be viewed in the online issue, which is available at wileyonlinelibrary.com.]

In the sb-L15-2 diblock copolymer, the PDLA block was slightly shorter than the PLLA segment. When it blended with L15, two stereocomplex formats could form. However, the PLLA block and PDLA segment would stereocomplex through inter or intramolecular interaction. However, the stereocomplexation could form between PDLA block and L15 molecule. In this binary blend, the structure of PLLA block was identical to L15; thus, the T_{sc} of sb-L15-2/L15 mainly depended on the PDLA block, so the T_{sc} was not changed obviously weather it blended with L15 or not. However, in the sb-L15-2/D14, both the D14 and PDLA block could stereocomplex with the PLLA block, but the D14 had higher mobility, and its molecular weight was more symmetrical with the PLLA block. Accordingly, the stereocomplexation mainly formed between D14 and PLLA segment, and resulted in a higher T_{sc}.

The WAXD of these specimens is shown in Figure 3(b). The diffraction peaks at 12.0, 21.0, and 24.1° assigned to PLA sc is clearly observed in all specimens. After sb-L15-2 blended with L15, another diffraction peak at 16.9° was detected, which should be due to the formation of PLA hc.[6,15,37,44] In

the sb-L15-2/D14, the intensity of diffraction peak at 16.9° became broader and weaker, but in the DSC measurement, no PLA hc was found during heating; this indicates that the WAXD was more sensitive than the DSC measurement.

Sb-4L60-2/PLAs

The thermal property of sb-4L60-2/PLA blends is seen in Figure 4(a), and the data is collected in Table 3. The sb-4L60-2 melted at 204.5 °C; after blending with L15, an exothermic peak appeared at 210.4 °C. In the sb-4L60-2/D14, apart from the peak at exothermic 214.5 °C, another weak peak around 160 °C was observed. The peak above 200 °C indicated the melting of PLA sc, and the peak at 160 °C was ascribed to PLA hc. The WAXD of the samples is listed in Figure 4(b), all specimens showed obvious diffraction peaks assigned to PLA sc, and only a wide and weak diffraction peak at 16.9° was observed in the sb-4L60-2/D14 specimen.

In the sb-L15-2/PLA blends, the T_{sc} in sb-L15-2/L15 was similar to that of neat copolymer, which should be ascribed to the shorter PDLA block, and the stereocomplex formation between PLLA block and PDLA block and between L15 and PDLA block were similar. However, the temperature in sb-L15-2/D14 was higher than the neat copolymer, which indicated that the stereocomplex formation between PLLA block and D14 was the major formation in this specimen. In addition, the residual PLLA block or PDLA block in these two binary blends could aggregate and form a small amount of PLA hc due to their strong mobility. In the sb-4L60-2/PLA specimens, the T_{sc} in sb-4L60-2/L15 blend was higher than that of sb-4L60-2, and that temperature was the highest in the sb-4L60-2/D14 sample, due to the fact that the stereocomplexation between PLLA and PDLA blocks in sb-4L60-2 was restrained by the steric hindrance from the four-armed structure. After the free PLA molecule was added, it could stereocomplex with PDLA or PLLA block more efficiently, and the T_{sc} was enhanced. Compared to the PDLA block in the sb-4L60-2, the PLLA branch in the copolymer was more uniform, which resulted in the higher T_{sc} in sb-4L60-2/D14.

This phenomenon strongly suggested that in the copolymer/ PLAs specimens, the stereocomplex formation between PLLA or PDLA block and free enantiomeric PLA molecule was the major formation. Moreover, the T_{sc} in copolymer/D-configuration blends was higher than corresponding L-configuration
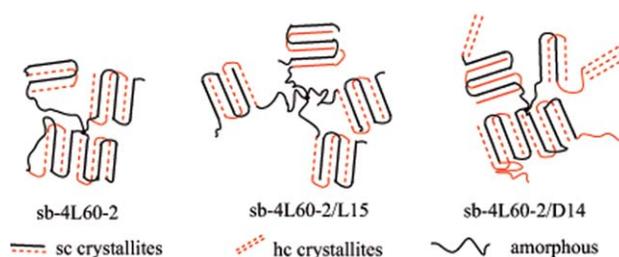
SCHEME 3 The crystallites formation of T_{sc} in sb-4L60-2 and its blends. [Color figure can be viewed in the online issue, which is available at wileyonlinelibrary.com.]
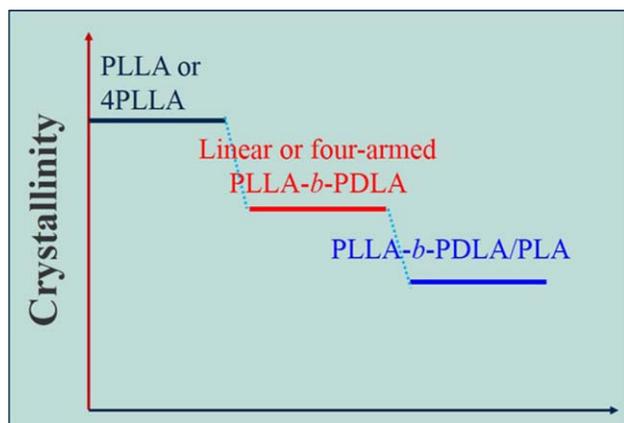
SCHEME 4 The crystallization of PLA prepolymer, copolymer, and blends. [Color figure can be viewed in the online issue, which is available at wileyonlinelibrary.com.]

specimens, which implied that the uniformity of the PDLA block was worse than the PLLA block, and reduced the stereocomplexation ability of PDLA block. In the sb-4L60-2/L15, the stereocomplexation formed between the PDLA block and L15, while the core inside and the sc outside confined the inside PLLA block; thus, it cannot form crystallites (Scheme 3). However, in the sb-4L60-2/D14, the stereocomplexation formed between inside PLLA block and D14, the outside PDLA block can develop some hc due to its relatively stronger mobility.

According to the calculated ΔH_{sc} in Table 3, the melting enthalpies of sc in the blends were smaller than corresponding neat copolymers. Two-thirds of PLA chains participated in the stereocomplex formation, and the stereocomplexation efficiency strengthened in all blends; this phenomenon was observed more obviously in sb-4L60-2/PLA specimens. However, one-third of the PLA block did not participate in the stereocomplex formation. The PLA hc in all the block copolymer/PLA specimens were suppressed, which would be due to the fact that preferentially formed PLA sc inhibited the growth of PLA hc, resulting in the decline of total crystallinity in all the blends.

The differences of crystallization behaviors among linear and four-armed PLLA, PLLA-*b*-PDLA block copolymer, and PLLA-*b*-PDLA/PLA blends in this study are illustrated in Scheme 4. In the linear or four-armed PLLAs, they could congregate and form PLA hc by themselves. In the block copolymers with similar length of PLLA and PDLA blocks, the PLLA block would stereocomplex with the PDLA block and form PLA sc. When the copolymers blended with PLAs, for example sb-L15-2/L15, the stereocomplexes could form between not only PLLA and PDLA blocks, but also between L15 and the PDLA block. Moreover, the surplus molecular chains would form some microcrystallites in some specimens. Thus, the crystallization of PLA sc and hc would compete and restrain reciprocally, which resulted in the reducing of total crystallinity in the blends. These results were similar to the ancient Chinese proverb "One monk will shoulder two buckets of

water (PLLA or 4PLLA), two monks will share the load (linear and four-armed PLLA-*b*-PDLA), but add a third and no one will want to fetch water (copolymer/PLA blends)."

CONCLUSIONS

In this study, the linear and four-armed PLLA-*b*-PDLA block copolymers were synthesized and their crystallization and melting behaviors were investigated. Results indicated that the melting temperature, crystallization temperature, and the corresponding enthalpies of stereocomplex crystallites in the copolymers were lower than those of linear and four-armed PLLA/PDLA blends, which was due to the restriction of chemical bonds between the PDLA and PLLA block in the block copolymers. The melting temperature and enthalpy of PLA stereocomplex decreased as the branched structure increased.

After the block copolymers blended with linear PLAs with different configurations, the DSC and WAXD results indicated that the stereocomplex formation between free PLA molecule and enantiomeric PLA block was the major formation. In the linear copolymer/PLA casted films, besides the stereocomplex crystallites, small amount of hc formed. However, in the four-armed copolymer/PLA blends, the hc formed only when the outside block did not participate in the stereocomplexation. Although the melting enthalpy of stereocomplexes in the blends was obviously lower than that in copolymers, the stereocomplex efficiency strengthened, but the crystallization of homochiral polymers and the total crystallininty were suppressed. This investigation will provide some information for the applications of PLLA-*b*-PDLA block copolymers.

REFERENCES AND NOTES

1 X. A. Pang, X. L. Zhuang, Z. H. Tang, X. S. Chen, *Biotechnol. J.* **2010**, *5*, 1125–1136.

2 K. Madhavan Nampoothiri, N. R. Nair, R. P. John, *Bioresour. Technol.* **2010**, *101*, 8493–8501.

3 S. Inkinen, M. Hakkarainen, A. C. Albertsson, A. Sodergard, *Biomacromolecules* **2011**, *12*, 523–532.

4 J. M. Becker, R. J. Pounder, A. P. Dove, *Macromol. Rapid Commun.* **2010**, *31*, 1923–1937.

5 H. Liu, J. Zhang, *J. Polym. Sci. Part B: Polym. Phys.* **2011**, *49*, 1051–1083.

6 Y. Ikada, K. Jamshidi, H. Tsuji, S. H. Hyon, *Macromolecules* **1987**, *20*, 904–906.

7 H. Tsuji, *Macromol. Biosci.* **2005**, *5*, 569–597.

8 K. Fukushima, Y. Kimura, *Polym. Int.* **2006**, *55*, 626–642.

9 H. Tsuji, S. H. Hyon, Y. Ikada, *Macromolecules* **1991**, *24*, 5651–5656.

10 H. Tsuji, S. H. Hyon, Y. Ikada, *Macromolecules* **1991**, *24*, 5657–5662.

11 Y. Liu, J. Sun, X. Bian, L. Feng, S. Xiang, B. Sun, Z. Chen, G. Li, X. Chen, *Polym. Degrad. Stab.* **2013**, *98*, 844–852.

12 J. Sun, J. Shao, S. Huang, B. Zhang, G. Li, X. Wang, X. Chen, *Mater. Lett.* **2012**, *89*, 169–171.

13 T. Biela, A. Duda, S. Penczek, *Macromolecules* **2006**, *39*, 3710–3713.

14 T. Biela, *Polimery* **2007**, *52*, 106–116.

15 J. Shao, J. Sun, X. Bian, Y. Cui, G. Li, X. Chen, *J. Phys. Chem. B* **2012**, *116*, 9983–9991.

16 P. Purnama, S. H. Kim, *Macromolecules* **2010**, *43*, 1137–1142.

17 P. Purnama, S. H. Kim, *Polym. Int.* **2012**, *61*, 939–942.

18 K. Fukushima, Y. H. Chang, Y. Kimura, *Macromol. Biosci.* **2007**, *7*, 829–835.

19 M. Hirata, K. Kobayashi, Y. Kimura, *J. Polym. Sci. Part: A Polym. Chem.* **2010**, *48*, 794–801.

20 H. Tsuji, T. Wada, Y. Sakamoto, Y. Sugiura, *Polymer* **2010**, *51*, 4937–4947.

21 L. B. Li, Z. Y. Zhong, W. H. de Jeu, P. J. Dijkstra, J. Feijen, *Macromolecules* **2004**, *37*, 8641–8646.

22 K. Masutani, C. W. Lee, Y. Kimura, *Macromol. Chem. Phys.* **2012**, *213*, 695–704.

23 K. Masutani, S. Kawabata, T. Aoki, Y. Kimura, *Polym. Int.* **2010**, *59*, 1526–1530.

24 S. I. Moon, I. Taniguchi, M. Miyamoto, Y. Kimura, C. W. Lee, *High Perform. Polym.* **2001**, *13*, S189–S196.

25 K. Fukushima, M. Hirata, Y. Kimura, *Macromolecules* **2007**, *40*, 3049–3055.

26 Z. Tang, X. Chen, X. Pang, Y. Yang, X. Zhang, X. Jing, *Biomacromolecules* **2004**, *5*, 965–970.

27 Z. H. Tang, X. S. Chen, Y. K. Yang, X. Pang, J. R. Sun, X. F. Zhang, X. B. Jing, *J. Polym. Sci. Part A: Polym. Chem.* **2004**, *42*, 5974–5982.

28 N. Sugai, T. Yamamoto, Y. Tezuka, *ACS Macro Lett.* **2012**, *1*, 902–906.

29 A. Hirao, H.-S. Yoo, *Polym. J.* **2011**, *43*, 2–17.

30 X. Zhu, Y. Zhou, D. Yan, *J. Polym. Sci. Part B Polym. Phys.* **2011**, *49*, 1277–1286.

31 I. Arvanitoyannis, A. Nakayama, N. Kawasaki, N. Yamamoto, *Polymer* **1995**, *36*, 2947–2956.

32 F. Tasaka, Y. Ohya, T. Ouchi, *Macromolecules* **2001**, *34*, 5494–5500.

33 Q. Cai, Y. Zhao, J. Bei, F. Xi, S. Wang, *Biomacromolecules* **2003**, *4*, 828–834.

34 T. Biela, A. Duda, K. Rode, H. Pasch, *Polymer* **2003**, *44*, 1851–1860.

35 Y. Sakamoto, H. Tsuji, *Macromol. Chem. Phys.* **2013**, *214*, 776–786.

36 S. Regnell Andersson, M. Hakkarainen, S. Inkinen, A. Södergård, A. C. Albertsson, *Biomacromolecules* **2012**, *13*, 1212–1222.

37 J. Shao, J. Sun, X. Bian, Y. Cui, Y. Zhou, G. Li, X. Chen, *Macromolecules* **2013**, *46*, 6963–6971.

38 S. Inkinen, M. Stolt, A. Sodergard, *Polym. Adv. Technol.* **2011**, *22*, 1658–1664.

39 T. Isono, Y. Kondo, I. Otsuka, Y. Nishiyama, R. Borsali, T. Kakuchi, T. Satoh, *Macromolecules* **2013**, *46*, 8509–8518.

40 H. R. Kricheldorf, I. Kreisersaunders, C. Boettcher, *Polymer* **1995**, *36*, 1253–1259.

41 S. H. Kim, Y.-K. Han, Y. H. Kim, S. I. Hong, *Die Makromol. Chem.* **1992**, *193*, 1623–1631.

42 S. H. Kim, Y. K. Han, K. D. Ahn, Y. H. Kim, T. Chang, *Makromol. Chem.-Macromol. Chem. Phys.* **1993**, *194*, 3229–3236.

43 J. M. Zhang, H. Sato, H. Tsuji, I. Noda, Y. Ozaki, *Macromolecules* **2005**, *38*, 1822–1828.

44 J. Shao, J. Sun, X. Bian, Y. Zhou, G. Li, X. Chen, *CrystEngComm* **2013**, *15*, 6469–6476.